ELSEVIER

Journal of Alloys and Compounds 338 (2002) 26–31

Journal of ALLOYS AND COMPOUNDS

www.elsevier.com/locate/jallcom

Crystal growth and co-substitution in $(Mg_{1-x}Fe_x)(Mo_{2-x}V_x)O_7$ $(0.13 \leq x \leq 0.47)$ with (V/Mo)=O oxo double bonds ☆

Xiandong Wang, Alexander J. Norquist, Jason Pless, Charlotte L. Stern, Douglas A. Vander Griend, Kenneth R. Poeppelmeier*

Department of Chemistry, Northwestern University, Evanston, IL 60208-3113, USA

Received 12 September 2001; accepted 8 December 2001

Abstract

New solid solution crystals of $(Mg_{1-x}Fe_x)(Mo_{2-x}V_x)O_7$ $(0.13 \leq x \leq 0.47)$ were grown from $MgO–Fe_2O_3–V_2O_5–MoO_3$ melts. Single crystal X-ray diffraction studies reveal that the structure consists of $(Mg/Fe)_2O_{10}$ octahedral dimers and $[(Mo_{2-x}V_x)O_7]^{(2+x)-}$ tetrahedral clusters. The structure contains (V/Mo)=O oxo double bonds similar to $MgMo_2O_7$ and $FeVMoO_7$. Equimolar co-substitution of V^{5+} for Mo^{6+} and Fe^{3+} for Mg^{2+} avoids the creation of any ion vacancies or interstitials and generates disordered cation sites. Crystal data: for $(Mg_{0.87}Fe_{0.13})(Mo_{1.87}V_{0.13})O_7$, monoclinic, space group $P2_1/n$ (No. 14), with $a=8.3356(6)$ Å, $b=9.1079(6)$ Å, $c=8.5086(6)$ Å, $\beta=111.927(1)°$ and $Z=4$; for $(Mg_{0.53}Fe_{0.47})(Mo_{1.53}V_{0.47})O_7$, monoclinic, space group $P2_1/n$ (No. 14), with $a=8.2766(6)$ Å, $b=9.0208(7)$ Å, $c=8.4817(6)$ Å, $\beta=112.144(1)°$ and $Z=4$.

Keywords: Molybdate; Vanadate; Crystal growth; Metal oxo double bond

1. Introduction

Vanadates and molybdates are widely used as catalysts for a variety of heterogeneous catalytic reactions. The binary oxide catalysts $SbVO_4$ and $(VO)_2P_2O_7$ are both used industrially. More complex systems have also proven fruitful. Ternary phase diagrams can be explored thoroughly with a reasonable number of polycrystalline and single crystal syntheses. Recently, during the investigation of the $MgO–V_2O_5–MoO_3$, $Fe_2O_3–V_2O_5–MoO_3$ and $MgO–Fe_2O_3–V_2O_5$ systems, several ternary compounds such as $Mg_{2.5}VMoO_8$ [1], $Fe_2V_3MoO_{13.5}$ [2], $FeVMoO_7$ [3], $Fe_4V_2Mo_3O_{20}$ [4] and $FeMg_2V_3O_{11}$ [5], were found by powder X-ray diffraction (XRD) and then fully characterized by single crystal XRD. In the $MgO–Fe_2O_3–MoO_3$ system no ternary compounds were reported. Possibilities scale with complexity, but the number of combinations makes the blind exploration of quaternary space daunting. Discovery of more complex oxides can be facilitated by single crystal growth from rationally chosen melts. Explorative crystal growth can pinpoint thermodynamic products, delineate substitution mechanisms, and elucidate phase diagrams. Complete characterization of single crystal products is also much more straightforward. The quaternary $MgO–Fe_2O_3–V_2O_5–MoO_3$ system was investigated based upon knowledge of the four ternary systems. Compositions with a comparable number of low and high valent cations will most likely form structures with isolated tetrahedra for the latter. Previous studies also revealed an interesting structural evolution from $Mg_2Mo_4O_{14}$ to $Fe_2V_2Mo_2O_{14}$, and then to $Fe_2V_3MoO_{13.5}$, and finally to $Fe_2V_4O_{13}$ [2]. $MgMo_2O_7$ contains rare Mo=O oxo double bonds [6]. Based on the structural similarities of these four compounds, $Mg_2FeVMo_5O_{21}$ on the $MgMo_2O_7–FeV–MoO_7$ tie line and $MgFeV_2Mo_2O_{13.5}$ on the $Fe_2V_4O_{13}–MgMo_2O_7$ tie line were targeted as promising compositions for new vanadomolybdates.

2. Experimental

2.1. Crystal growth

MgO (99.9%, Aldrich), Fe_2O_3 (99%, Aldrich), V_2O_5 (99.6%, Aldrich), MoO_3 (99.5%, Aldrich) were used for all syntheses. A 8.275-g amount of composition A with a

☆In honor of Fritz Franzen.

*Corresponding author. Fax: +1-847-491-7713.

E-mail address: krp@northwestern.edu (K.R. Poeppelmeier).

0925-8388/02/$ – see front matter
PII: S0925-8388(02)00178-0

nominal composition of $Mg_2FeV_{1.94}Mo_{9.72}O_{37.51}$ was ground in an agate mortar and heated at 500 °C for 4 h to remove moisture. The mixed powder was then pressed into pellets, placed in a fused-silica tube in air, evacuated and sealed. The quartz tube was tilted about 20° and heated to 800 °C for 2 h at 180 °C h^{-1} in the constant temperature zone of a tube furnace, cooled slowly to 600 °C at 6 °C h^{-1}, and further cooled to room temperature at 120 °C h^{-1}. This composition, which was originally designed to search for the predicted $Mg_2FeVMo_5O_{21}$ compound, yielded three different types of crystals: orange-red prismatic crystals of unknown stoichiometry (**X1**), light green platelet crystals and orange prismatic crystals. The latter two were readily identified as $Fe_2(MoO_4)_3$ and $MgMoO_4$, respectively.

A 7.00-g amount of composition B with a nominal stoichiometry of $MgFeV_{5.78}Mo_{5.78}O_{34.29}$ was ground, pressed into a pellet and sealed in a quartz tube. The sample was then heated to 750 °C for 5 h at 180 °C h^{-1}, cooled slowly to 500 °C at 6 °C h^{-1}, and further cooled to room temperature at 120 °C/h. Green-yellow rectangular thin platelet crystals (**X2**) were retrieved from the flux, but a longitudinal line in the middle of each crystal observed under plane polarized light indicated the existence of twinning. Preliminary studies by single crystal XRD confirmed this result.

The composition was modified to $MgFeV_{4.67}Mo_{4.67}O_{28.19}$ to prepare composition C, and the same experimental conditions used for composition B were adopted except for the last cooling step, that is 60 °C/h instead of 120 °C/h. Green-yellow rectangular thin platelet crystals (**X3**) again were obtained, some of which did not exhibit multiple domains under a polarized light optical microscope or peak splitting in the ω-scan profile.

2.2. Analysis

The crystals grown from A, B and C were analyzed by energy dispersive analysis of X-rays (EDAX) using pure phases of $FeVMoO_7$ and $FeMg_2V_3O_{11}$ as standards for composition calibration. The atomic ratios of Mg:Fe:Mo:V for the **X1**, **X2** and **X3** crystals were analyzed by EDAX to be 0.91:0.09:1.78:0.09, 0.73:0.27:1.51:0.31 and 0.61:0.39:1.38:0.42, respectively. Inductively coupled plasma atomic emission spectrophotometry (ICP-AES, Thermo Jarrell Ash, model Atomscan 25) was also used to determine composition. Each compound was dissolved in aqua regia and diluted with deionized water. The average atomic ratios of Mg:Fe:Mo:V for **X1**, **X2** and **X3** crystals were analyzed by ICP to be 0.82:0.18:2.18:0.11, 0.66:0.34:1.07:0.20 and 0.54:0.46:1.76:0.42, respectively. Low concentrations of vanadium result from the significant interference of the V (290.877 nm) line with the Mo (290.912 nm) line. Assuming these compositions lie along the $Mg_{1-x}Fe_xMo_{2-x}V_xO_7$ line then these results indicate compositions of $Mg_{0.86}Fe_{0.14}Mo_{1.86}V_{0.14}O_7$ ($x=0.14$), $Mg_{0.66}Fe_{0.34}Mo_{1.66}V_{0.34}O_7$ ($x=0.34$), and $Mg_{0.54}Fe_{0.46}Mo_{1.54}V_{0.46}O_7$ ($x=0.46$) for crystals **X1**, **X2**, and **X3**, respectively.

2.3. Crystallographic determination

Crystals **X1** and **X3** were not twinned and could be refined from single crystal XRD data. An orange **X1** crystal (0.13 mm×0.09 mm×0.06 mm) cut from a rectangular prism and a thin green platelet **X3** crystal (0.18 mm×0.16 mm×0.02 mm) were mounted on glass fibers and investigated with a Smart 1000 Bruker diffractometer with CCD detector. The short, midlength, and long dimensions of the **X3** crystal were determined to be the [010], [100] and [001] directions, respectively. Systematic extinctions ($h0l$, $l\neq 2n$; $0k0$, $k\neq 2n$) unambiguously establish $P2_1/n$ (No. 14) as the correct space group for both unknown crystals. The possibility of crystal twinning was meticulously eliminated. An analytical absorption correction resulted in transmission factor ranges of 0.54–0.78 for **X1** and 0.37–0.90 for **X3**. All calculations were performed using TEXSAN crystallographic software package from Molecular Structure [7]. The structures were solved by direct methods [8] and expanded using Fourier techniques [9].

All three cation sites within the structure are disordered: two for vanadium and molybdenum, and one for iron and magnesium. The reported formulae were determined under the assumption that every atomic site is fully occupied. Every value of x between 0 and 1 resulted in an acceptable refinement, but when x was fixed to 0.128 for **X1** and 0.467 for **X3**, R and R_w values approached minima, in excellent agreement with the analyzed compositions. All atoms were refined using anisotropic thermal parameters except for the disordered ones. Additional crystallographic data, selected atomic coordinates, and selected bond lengths and angles are listed in Tables 1–4 and in the Supplemental information.

3. Results and discussion

3.1. Composition

The existence of a co-substitution $(Mg_{1-x}Fe_x)(Mo_{2-x}V_x)O_7$ solid solution from $x=0.13$ to $x=0.47$ is confirmed by the isostructural compounds **X1** ($x=0.13$) ($P2_1/n$: $a=8.336(1)$ Å, $b=9.108(1)$ Å, $c=8.509(1)$ Å, $\beta=111.93(1)°$, $Z=4$) and **X3** ($x=0.47$) ($P2_1/n$: $a=8.277(1)$ Å, $b=9.021(1)$ Å, $c=8.482(1)$ Å, $\beta=112.14(1)°$, $Z=4$). $MgMo_2O_7$ ($P2_1/c$: $a=8.111(2)$ Å, $b=5.700(1)$ Å, $c=15.002(3)$ Å, $\beta=115.26(2)°$, $Z=4$) and $FeVMoO_7$, $a=5.564(1)$ Å, $b=6.669(1)$ Å, $c=7.909(1)$ Å, $\alpha=96.29(1)°$, $\beta=90.33(1)°$, $\gamma=101.32(2)°$, $Z=2$) could represent the $x=0$ and $x=1$ members of the title solution, respectively, but they are not isostructural with the solid solution [3,6]. Such peculiar intermediate compositions are

Table 1
Crystallographic data for $(Mg_{1-x}Fe_x)(Mo_{2-x}V_x)O_7$ (x=0.13 and 0.47)

Formula	$(Mg_{0.87}Fe_{0.13})(Mo_{1.87}V_{0.13})O_7$	$(Mg_{0.53}Fe_{0.47})(Mo_{1.53}V_{0.47})O_7$
Formula weight	326.43	321.86
Space group	$P2_1/n$ (No. 14)	$P2_1/n$ (No. 14)
a (Å)	8.3356(6)	8.2766(6)
b (Å)	9.1079(6)	9.0208(7)
c (Å)	8.5086(6)	8.4817(6)
β (°)	111.927(1)	112.144(1)
V (Å^3)	599.24(6)	586.55(7)
Z	4	4
T (°C)	−120	−120
λ (Å)	0.71069	0.71069
ρ_{calc} (g/cm^3)	3.62	3.64
μ (mm^{-1})	4.48	5.17
R^a	0.033	0.030
$R_w{}^b$	0.036	0.035

[a] $R=\Sigma\dfrac{|F_0|-|F_c|}{\Sigma|F_0|}$.

[b] $R_w=\left[\dfrac{\Sigma w(|F_0|-|F_c|)^2}{\Sigma w|F_0|^2}\right]^{1/2}$.

Table 2
Atomic parameters for $(Mg_{0.87}Fe_{0.13})(Mo_{1.87}V_{0.13})O_7$

Atom	x	y	z	Occupancy
Mg(1)	0.9984(1)	0.4932(1)	0.8128(1)	0.872(3)
Fe(1)	0.9984(1)	0.4932(1)	0.8128(1)	0.128(3)
Mo(1)	0.63412(4)	0.36028(3)	0.84516(4)	0.916(1)
V(1)	0.63412(4)	0.36028(3)	0.84516(4)	0.084(1)
Mo(2)	0.30012(4)	0.61852(3)	0.60602(3)	0.956(1)
V(2)	0.30012(4)	0.61852(3)	0.60602(3)	0.044(1)
O(1)	0.5482(3)	0.3363(2)	0.9936(3)	1.0
O(2)	0.4869(3)	0.4913(3)	0.6844(3)	1.0
O(3)	0.3696(3)	0.7987(2)	0.6477(3)	1.0
O(4)	0.2030(3)	0.5937(2)	0.3873(3)	1.0
O(5)	0.1508(3)	0.5725(2)	0.0475(3)	1.0
O(6)	0.1530(3)	0.5714(2)	0.6960(3)	1.0
O(7)	0.1317(3)	0.3099(2)	0.2527(3)	1.0

Table 3
Atomic parameters for $(Mg_{0.53}Fe_{0.47})(Mo_{1.53}V_{0.47})O_7$

Atom	x	y	z	Occupancy
Mg(1)	0.99838(8)	0.49509(7)	0.81397(7)	0.534(3)
Fe(1)	0.99838(8)	0.49509(7)	0.81397(7)	0.466(3)
Mo(1)	0.63268(4)	0.36011(3)	0.84262(4)	0.683(1)
V(1)	0.63268(4)	0.36011(3)	0.84262(4)	0.317(1)
Mo(2)	0.29917(3)	0.61865(3)	0.60690(3)	0.850(1)
V(2)	0.29917(3)	0.61865(3)	0.60690(3)	0.150(1)
O(1)	0.5479(3)	0.3348(2)	0.9907(3)	1.0
O(2)	0.4863(3)	0.4923(2)	0.6837(2)	1.0
O(3)	0.3705(2)	0.7989(2)	0.6478(2)	1.0
O(4)	0.1989(3)	0.5928(2)	0.3871(2)	1.0
O(5)	0.1486(2)	0.5716(2)	0.0481(2)	1.0
O(6)	0.1529(2)	0.5703(2)	0.6977(2)	1.0
O(7)	0.1289(2)	0.3090(2)	0.2474(2)	1.0

potentially difficult to discover owing to the lack of direct structural ties with more simple stoichiometries. It is also a non-trivial matter to explain the solubility limits in this case given that both the x=0 and x=1 members exist. It is even difficult to ascertain whether compositions within the ranges $0.0<x<0.13$ and $0.47<x<1.0$ would form single phases or not.

Regardless of starting composition, the crystalline products exhibit ratios of low valent cations to high valent cations to anions of 1 to 2 to 7. The starting ratio of molybdenum to vanadium was always less than that of the final crystal for all three starting compositions. For composition A, the low starting vanadium concentration allows an x of only 0.13 despite enough iron to achieve x=0.33. Both compositions B and C contain equal amounts of Fe^{3+} and Mg^{2+} along with equal amounts of V^{5+} and Mo^{6+}, so crystals with x=0.5 seem most appropriate. They produce crystals where that fraction has decreased to x=0.35 and 0.47, respectively. Perhaps increasing the amount of vanadium and molybdenum still further would increase x. If MoO_3 is more volatile than V_2O_5, then simply increasing the amount of vanadium would also accomplish this. In general, it appears as if a particular x could be best achieved by choosing a flux composition with the targeted ratio of iron and magnesium and a large excess of vanadium and molybdenum.

The co-substitution mechanism $(Mg_{1-x}Fe_x)(Mo_{2-x}V_x)O_7$ does not create any ion vacancies or interstitials. This is in contrast to previously reported ternary solid solutions $Mg_{2+x}V_{2x}Mo_{2-2x}O_8$ ($x\leq1$) [1] and $Fe_2V_{3+x}Mo_{1-x}O_{13.5-x/2}$ ($x\leq0.16$) [2]. The present substitution mechanism is similar to $Fe_{4-x}Mg_xV_{2-x}Mo_{3+x}O_{20}$ ($x\leq1.59$) [4].

Table 4
Selected bond lengths, angles and differences for $(Mg_{1-x}Fe_x)(Mo_{2-x}V_x)O_7$

	Bond lengths (Å)				Bond angles (°)		
	$x=0.13$	$x=0.47$	Δ		$x=0.13$	$x=0.47$	Δ
Mg/Fe(1)–O3	2.046(4)	2.037(3)	0.009	O1–Mo/V(1)–O2	106.4(2)	106.8(2)	−0.4
Mg/Fe(1)–O4	2.052(4)	2.025(3)	0.027	O1–Mo/V(1)–O5	106.7(2)	106.6(1)	0.1
Mg/Fe(1)–O5	2.056(4)	2.026(3)	0.030	O1–Mo/V(1)–O7	106.8(2)	107.0(2)	−0.2
Mg/Fe(1)–O5	2.103(4)	2.069(3)	0.034	O2–Mo/V(1)–O5	114.3(2)	113.9(1)	0.4
Mg/Fe(1)–O6	2.028(4)	2.004(3)	0.024	O2–Mo/V(1)–O7	110.0(2)	109.6(1)	0.4
Mg/Fe(1)–O7	2.062(4)	2.022(3)	0.040	O5–Mo/V(1)–O7	112.2(2)	112.4(1)	−0.2
Mo/V(1)–O1	1.683(4)	1.669(3)	0.014	O2–Mo/V(2)–O3	110.3(2)	109.6(1)	0.7
Mo/V(1)–O2	1.884(4)	1.864(3)	0.020	O2–Mo/V(2)–O4	107.2(2)	107.7(1)	−0.5
Mo/V(1)–O5	1.789(4)	1.803(3)	−0.014	O2–Mo/V(2)–O6	109.0(2)	109.1(1)	−0.1
Mo/V(1)–O7	1.735(4)	1.721(3)	0.014	O3–Mo/V(2)–O4	109.1(2)	109.3(1)	−0.2
Mo/V(2)–O2	1.853(4)	1.834(3)	0.019	O3–Mo/V(2)–O6	112.6(2)	113.3(1)	−0.7
Mo/V(2)–O3	1.732(4)	1.720(3)	0.012	O4–Mo/V(2)–O6	108.5(2)	108.2(1)	0.3
Mo/V(2)–O4	1.745(4)	1.747(3)	−0.014				
Mo/V(2)–O6	1.725(4)	1.719(3)	0.006				

3.2. Structure

The $(Mg_{1-x}Fe_x)(Mo_{2-x}V_x)O_7$ ($x=0.13$, 0.47) structure consists of columns of edge-shared $(Mg/Fe)_2O_{10}$ octahedral dimers and corner-shared $(Mo/V)_2O_7$ tetrahedral clusters running in the *c* direction (see Fig. 1). Neighboring columns also share corners to form a three-dimensional network. Exactly one oxygen per formula unit (O1) is only bonded to one Mo/V atom forming a rare (Mo/V)=O oxo double bond [3]. The Mo/V(1)O_4 tetrahedra consist of two bicoordinate oxygens, one tricoordinate oxygen, and a unicoordinate oxygen (see Fig. 2). The bond lengths in Table 3 reflect this arrangement. Similar coordinating environments for MoO_4 exist in $MgMo_2O_7$ [6] and $FeVMoO_7$ [3].

Although $MgMo_2O_7$ ($x=0$) and $FeVMoO_7$ ($x=1$) are structurally similar to the title solid solution, the three compounds are not isostructural. Firstly, the arrangement of the octahedral units shown in Fig. 3 are different. Mg_2O_{10} units in $MgMo_2O_7$ arrange in a herringbone (see Fig. 3a). In contrast, the $(Mg/Fe)_2O_{10}$ units in the title solution align in parallel with a rotation between chains (see Fig. 3b). The Fe_2O_{10} units in $FeVMoO_7$ also align in parallel but without rotation (see Fig. 3c). Secondly, Fig. 4 clearly shows the different arrangements of the tetrahedral clusters within one unit cell for the three compounds. A

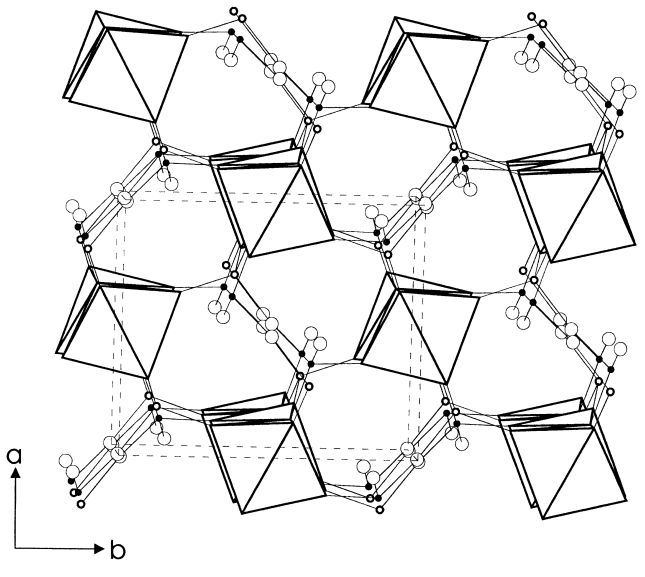

Fig. 1. Structure of $(Mg_{1-x}Fe_x)(Mo_{2-x}V_x)O_7$ ($0.13\leq x\leq 0.47$): (Fe/Mg)O_6, octahedra; Mo/V(1), small solid circle; Mo/V(2), small open circle; O, big open circle.

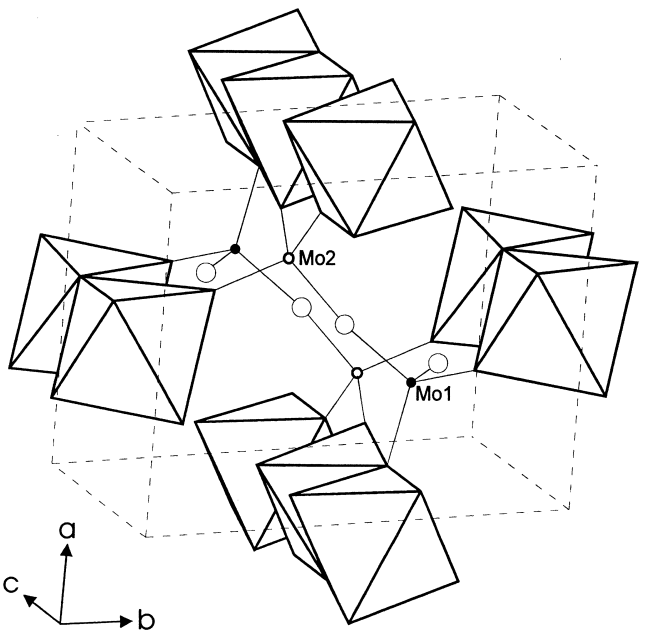

Fig. 2. Connections of tetrahedral clusters with octahedral dimers in $(Mg_{1-x}Fe_x)(Mo_{2-x}V_x)O_7$ ($0.13\leq x\leq 0.47$).

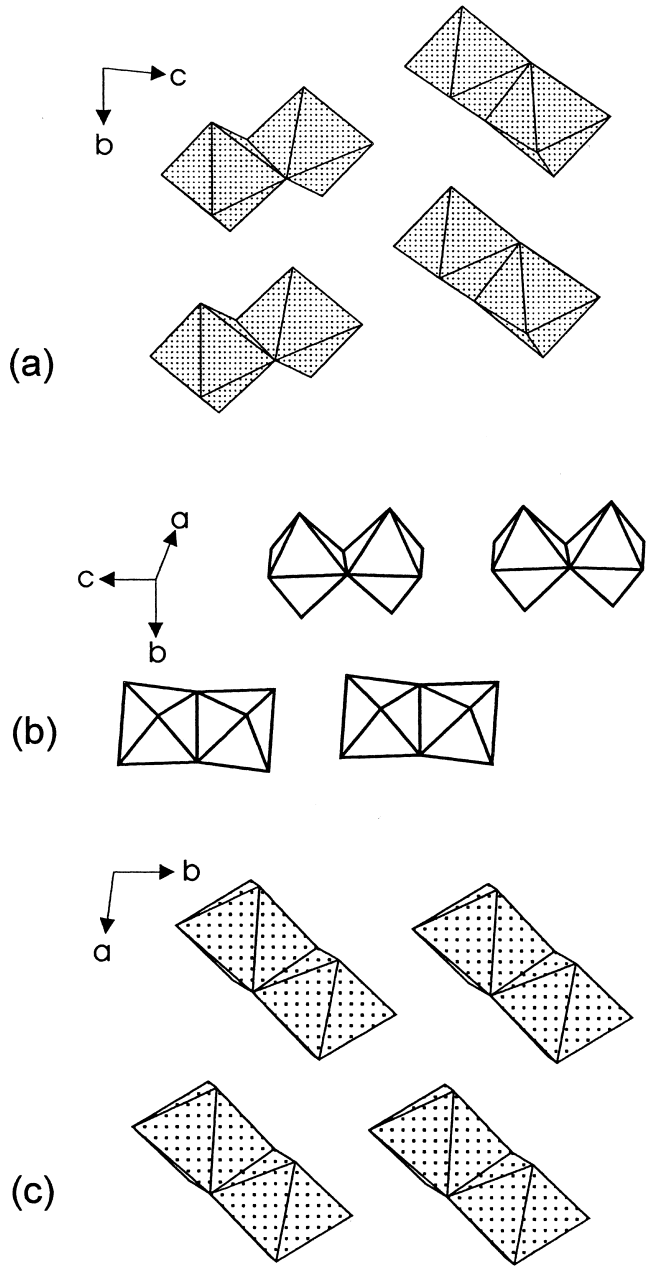

Fig. 3. Orientation comparison of the isolated M_2O_{10} units: (a) $MgMo_2O_7$; (b) $(Mg_{1-x}Fe_x)(Mo_{2-x}V_x)O_7$ $(0.13 \leq x \leq 0.47)$; (c) $FeVMoO_7$.

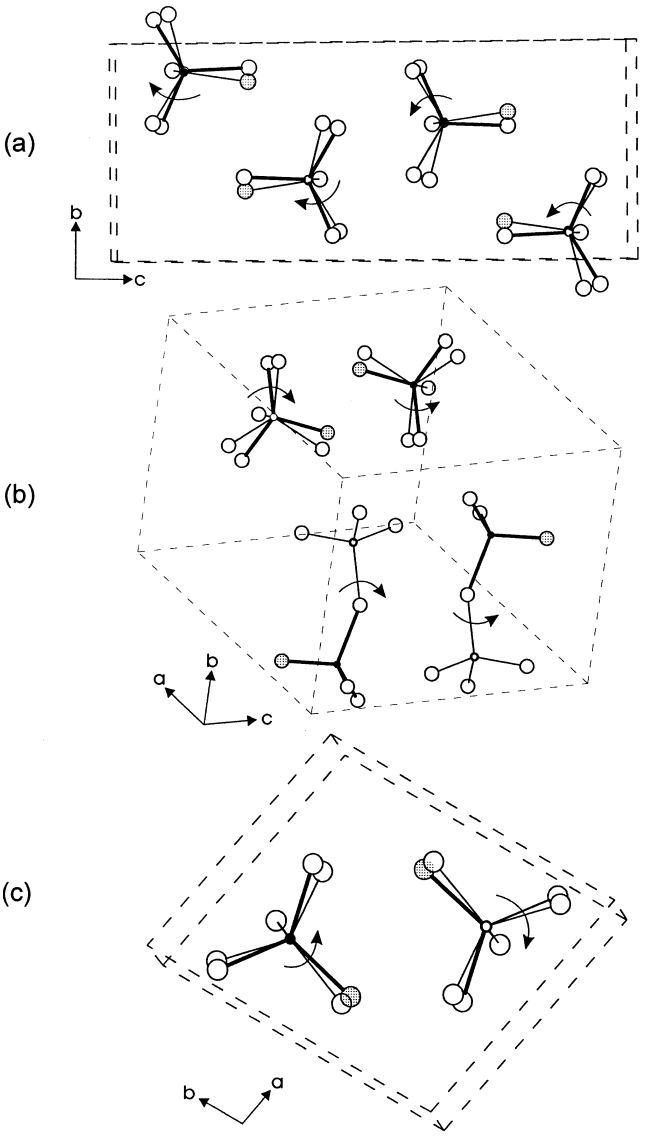

Fig. 4. Comparison of tetrahedral clusters: (a) $MgMo_2O_7$; (b) $(Mg_{1-x}Fe_x)(Mo_{2-x}V_x)O_7$ $(0.13 \leq x \leq 0.47)$ (origin of unit cell is shifted compared to Fig. 2); (c) $FeVMoO_7$. Arrows show the Newman projections of the tetrahedral clusters.

Newman projection along the two Mo/V ions for each cluster shows that all the clusters have nearly eclipsed conformation, with half skewed clockwise and the other half counterclockwise. The two different alignments of tetrahedral clusters in the solid solution are correlated with the alternating orientations of the octahedral columns.

As expected, the average (Mg/Fe)–O bond length of **X3** (2.031 Å) is between the average Mg–O bond (2.065 Å) in $MgMo_2O_7$ and the average Fe–O bond (1.992 Å) in $FeVMoO_7$. Nevertheless, the (V/Mo)=O bond length (1.669 Å) is even shorter than the Mo=O bonds in $MgMo_2O_7$ (1.707(4) Å) and $FeVMoO_7$ (1.689(4) Å), which is attributed to the presence of the smaller V^{5+} cation on the site with Mo^{6+}. Notably, the vanadium occupation on this site is approximately twice that of the Mo/V(2) site for both the **X1** and **X3** crystals.

3.3. Mo=O oxo bond

Surface V=O or Mo=O oxo groups in vanadate/molybdate catalysts play an important role for many heterogeneous catalytic reactions. These species participate in catalytic reactions such as the oxidation of sulfur dioxide to sulfur trioxide over V_2O_5 [10], methanol oxidation to formaldehyde on MoO_3 [11] and ammoxidation of propylene to acrylonitrile on α-$Bi_2Mo_3O_{12}$ [12]. Bulk oxo-groups are considerably more rare, and no catalytic

reactions have been performed with this type of oxide except α-MoO_3, in which the Mo coordination is octahedral rather than tetrahedral [13]. It is expected that terminating oxygen anions should have higher local electron density than bridging ones. However, surface terminal oxo-groups M=O and μ oxo-groups M–O–M are sufficiently nucleophilic to selectively oxidize C–H bonds [14]. $(Mg_{1-x}Fe_x)(Mo_{2-x}V_x)O_7$ (x=0, 0.13–0.47 and 1) contain both V/Mo=O and V/Mo–O–V/Mo groups in the bulk, and consequently provides a unique opportunity to study the catalytic mechanisms for hydrocarbon oxidation. Further investigations are needed to correlate the properties of bulk and surface oxo species.

3.4. Crystal twinning

There is a natural tendency to form twinned **X2** crystals because the production of twinned crystals from composition C was demonstrably repeatable. The *bc*-plane is most likely the twin boundary according to the observation of polarized optical microscope, assuming that **X2** and **X3** crystals have the same surface orientations. A similar twinning problem was encountered for the crystal growth of ferric molybdate $Fe_2(MoO_4)_3$ [15,16], in which the *ac*-plane was the twin boundary in the monoclinic $Fe_2(MoO_4)_3$ (space group $P2_1/a$, a=15.707 Å, b=9.231 Å, c=18.204 Å, β=125.25°). Twinned $Fe_2(MoO_4)_3$ crystal can lead to an incorrect space group determination, thus twin-free crystals are vital for structural determination. The influence of experimental conditions on the presence of twinned domains remains an intriguing question.

4. Conclusions

A new quaternary solid solution compound with rare V/Mo=O oxo double bonds $(Mg_{1-x}Fe_x)(Mo_{2-x}V_x)O_7$ ($0.13 \leq x \leq 0.47$) has been discovered in the $MgO–Fe_2O_3–V_2O_5–MoO_3$ system through single crystal growth. Its structure was investigated by X-ray single crystal diffraction and compared in detail with those of $FeVMoO_7$ and $MgMo_2O_7$.

5. Supplemental information

The supplementary material has been sent to Fach informationzentrum Karlsruhe, Abt. PROKA, 76344 Eggenstein-Leopoldshafen, Germany, as Supplementary material No. CSD-412271 (x=0.13) and CSD-412272 (x=0.47) and can be obtained by contacting the FIZ and quoting the article details and corresponding CSD number.

Acknowledgements

The authors thank Dr. Larry Cirjak and acknowledge a Research Award from BP America. This work was also supported by the National Science Foundation, Solid State Chemistry (DMR-9412971 and DMR-9727516) and made use of the Central Facilities supported by MRSEC program of the National Science Foundation (DMR-0076097) at the Materials Science Center of Northwestern University, and the EMSI program of the NSF and the Department of Energy (CHE-9810378) at the Northwestern University Institute for Environmental Catalysis.

References

[1] X. Wang, C.L. Stern, K.R. Poeppelmeier, J. Alloys Comp. 21 (1996) 51.
[2] X. Wang, K.R. Heier, C.L. Stern, K.R. Poeppelmeier, Inorg. Chem. 37 (1998) 6921.
[3] X. Wang, K.R. Heier, C.L. Stern, K.R. Poeppelmeier, Inorg. Chem. 37 (1998) 3252.
[4] X. Wang, A. Norquist, J. Pless, C.L. Stern, D.A. Vander Griend, K.R. Poeppelmeier, in preparation.
[5] X. Wang, D.A. Vander Griend, C.L. Stern, K.R. Poeppelmeier, J. Alloys Comp. 298 (2000) 119.
[6] K. Stadnicka, J. Haber, R. Kozlowski, Acta Cryst. 33 (1977) 3859.
[7] Crystal Structure Analysis Package, Molecular Structure, The Woodlands, TX, 1997.
[8] G.M. Sheldrick, SHELXS86, in: G.M. Sheldrick, C. Kruger, R. Goddard (Eds.), Crystallographic Computing 3, Oxford University Press, Oxford, 1985, pp. 175–189.
[9] P.T. Beurskens, G. Admiraal, G. Beuskens, W.P. Bosman, R. de Gelder, R. Israel, J.M.M. Smits, DIRDIF94, in: The DIRDIF-94 Program System; Technical Report of the Crystallographic Laboratory, University of Nijmegen, Nijmegen, 1994.
[10] J.P. Dunn, H.G. Stenger Jr., I.E. Wachs, Catalysis Today 51 (1999) 301.
[11] J.N. Allison, W.A. Goddard III, J. Catal. 92 (1985) 127.
[12] J.D. Burrington, C.T. Kartisek, R.K. Grasselli, J. Catal. 87 (1984) 363.
[13] L. Kihlborg, Ark Kemi 21 (1963) 357.
[14] J. Haber, T. Mlodnicka, J. Mol. Catal. 74 (1992) 131.
[15] M.H. Rapposch, J.B. Anderson, E. Kostiner, Inorg. Chem. 19 (1980) 3531.
[16] H.Y. Chen, Mat. Res. Bull. 14 (1979) 1583.